Binding Characteristics of a New Host Family of Cyclic Oligosaccharides from Inulin: Permethylated Cycloinulohexaose and Cycloinuloheptaose[1]

Yoshio Takai,† Yasuo Okumura,† Takanori Tanaka,† Masami Sawada,*,† Shigetoshi Takahashi,† Motoo Shiro,‡ Mishio Kawamura,§ and Takao Uchiyama*,§

Material Analysis Center, the Institute of Scientific and Industrial Research, Osaka University, Ibaraki, Osaka 567, Japan, Research Department, Rigaku Corporation, Akishima, Tokyo 196, Japan, and Department of Biology, Osaka Kyoiku University, Kashihara 582, Japan

Received December 10, 1993 (Revised Manuscript Received March 15, 1994•)

The complexation behavior of a new class of cyclic oligosaccharide hosts, permethylated cycloinulohexaose **1b** and permethylated cycloinuloheptaose **2b**, with various metallic cation guests has been characterized by means of FAB mass and NMR spectrometry and X-ray crystallography. A series of association constants (K_s) with metallic cations in acetone ($Li^+ < Na^+ < Cs^+ < K^+ < Ba^{2+}$) showed that **1b** acts like an 18-crown-6 derivative, but the binding abilities are lower by a factor of roughly 10^2 in the magnitude of K_s when compared with 18-crown-6 itself. Coupled with kinetic data (k_{-1}), charge-induced shift data, and low-temperature NMR signal splittings, as well as its cation selectivity pattern, the structure of the complex in solution was deduced such that the metallic cation is not captured by the central hole of the 18-crown-6 moiety of **1b** but is in the pocket constructed both by the upper rim OMe-3 oxygens of the furanose rings and by the crown ether oxygens. Unequivocal evidence for the OMe-3 participation in the cation binding of **1b** has been presented based on the crystalline structure of its barium cation complex [**1b**·Ba^{2+}].

Introduction

Cyclic oligosaccharides such as the cyclodextrin family have received a great deal of attention for a long time as principal skeletal compounds for novel hosts and artificial enzymes.[2] Most recently, another family of cyclic oligosaccharides (cyclofructans) have been prepared from inulin as cycloinulohexaose **1a**, cycloinuloheptaose **2a**, and cycloinulooctaose.[3-5]

The cyclodextrin family consists of cyclic oligosaccharides made of α-(1→4)-linked D-glucopyranose units, while the other cyclofructan family consists of β-(2→1)-linked D-fructofuranose units. The former compound has a cone-shaped cavity and can bind neutral molecules via hydrophobic interactions. In contrast, the latter has a characteristic crown ether skeleton in the central part of the molecule and is then expected to bind cationic molecules via charge-dipole electrostatic interactions. Indeed, complexation studies using ligand-exchange thin-layer chromatography,[5] etc.,[6] of **1a** and **2a** with various metallic cations in aqueous solution have shown the preference of K^+ (Ba^{2+}) and Cs^+ binding, respectively.

This paper describes the complexation studies of a new series of permethylated cyclofructans with cations. The thermodynamic and kinetic behavior of their complexations in organic solvents and the structures of their complex ions are treated. From the viewpoint of their binding abilities, selectivities, and complexing structures, one may regard the permethylated cyclofructans **1b** and **2b** as a new class of cation-binding macrocyclic hosts situated in positions next to the classes of crown ethers,[7] calixarenes,[8] and naturally occurring macrocyclic related compounds.[9] Stoddart and co-workers had extensively investigated the complexation behavior of synthetic chiral crown ethers into which certain carbohydrate molecules were incorporated as chiral barriers.[7d]

Results and Discussion

FAB Mass Spectral Analysis. FAB mass spectrometry (FABMS) is a sensitive probe of host–guest complex ions. In particular, it has been applied for the rapid screening of crown ether complexations with various cations.[10-12] We have detected complexation abilities[13] and enantioselectivities[14] of some carbohydrate hosts using the relative peak intensity (RPI) method and have demonstrated its applicability in a quantitative fashion. The RPI method basically uses an appropriate internal

† Osaka University.
‡ Rigaku Corporation.
§ Osaka Kyoiku University.
• Abstract published in *Advance ACS Abstracts*, April 15, 1994.

(1) Takai, Y.; Okumura, Y.; Takahashi, S.; Sawada, M.; Kawamura, M.; Uchiyama, T. *J. Chem. Soc., Chem. Commun.* **1993**, 53.

(2) For example: (a) Bender, M. L.; Komiyama, M. *Cyclodextrin Chemistry*; Springer-Verlag: New York, 1978. (b) Saenger, W. *Angew. Chem., Int. Ed. Engl.* **1980**, *19*, 344. (c) Tabushi, I. *Acc. Chem. Res.* **1982**, *15*, 66. (d) Breslow, R. *Science* **1982**, *218*, 532. (e) Clarke, R. J.; Coates, J. H.; Lincoln, S. F. *Adv. Carbohydr. Chem. Biochem.* **1988**, *46*, 205.

(3) (a) Kawamura, M.; Uchiyama, T.; Kuramoto, T.; Tamura, Y.; Mizutani, K. *Carbohydr. Res.* **1989**, *192*, 83. (b) Kawamura, M.; Uchiyama, T. *Biosci. Biotech. Biochem.* **1993**, *57*, 343.

(4) Sawada, M.; Tanaka, T.; Takai, Y. Hanafusa, T.; Taniguchi, T.; Kawamura, M.; Uchiyama, T. *Carbohydr. Res.* **1991**, *217*, 7.

(5) Uchiyama, T.; Kawamura, M.; Uragami, T.; Okuno, H. *Carbohydr. Res.* **1993**, *241*, 245.

(6) Yoshie, N.; Hamada, H.; Takada, S.; Inoue, S. *Chem. Lett.* **1993**, 353.

(7) For example: (a) Pedersen, C. J. *J. Am. Chem. Soc.* **1967**, *89*, 7017. (b) Cram, D. J. *Angew. Chem., Int. Ed. Engl.* **1988**, *27*, 1009. (c) Lehn, J.-M. *Angew. Chem., Int. Ed. Engl.* **1988**, *27*, 89. (d) Stoddart, J. F. *Chem. Soc. Rev.* **1979**, *8*, 85.

(8) For example: (a) Gutsche, C. D. *Acc. Chem. Res.* **1983**, *16*, 161. (b) Gutsche, C. D. In *Host Guest Complex Chemistry, Macrocycles*; Vögtle, F., Weber, E., Eds.; Springer-Verlag: Berlin, 1985; p 375. (c) Shinkai, S.; Manabe, O. *Nippon Kagaku Kaishi* **1988**, 1917.

(9) For example: Hilgenfeld, R.; Saenger, W. *Host Guest Complex Chemistry II*; Vögtle, F., Ed.; Springer-Verlag: Berlin, 1982; p 1.

(10) For example: (a) Medina, J. C.; Goodnow, T. T.; Rojas, M. T.; Atwood, J. L.; Lynn, B. C.; Kaifer, A. E.; Gokel, G. W. *J. Am. Chem. Soc.* **1992**, *114*, 10583. (b) Inokuchi, F.; Shiomi, Y.; Kawabata, H.; Sakaki, T.; Shinkai, S. *Chem. Lett.* **1993**, 1595.

(11) (a) Johnstone, R. A. W.; Lewis, I. A. S.; Rose, M. E. *Tetrahedron* **1983**, *39*, 1597. (b) Johnstone, R. A. W.; Rose, M. E. *J. Chem. Soc., Chem. Commun.* **1983**, 1268. (c) Johnstone, R. A. W.; Lewis, I. A. S. *Int. Mass Spectrom. Ion Phys.* **1983**, *46*, 451.

0022-3263/94/1959-2967$04.50/0

Chart 1

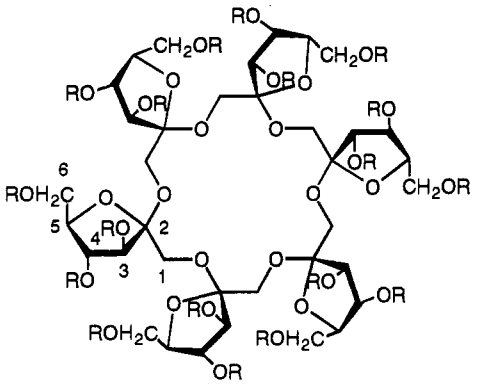

1

a : R = H
b : R = CH_3
c : R = CD_3
d : R = $COCH_3$
e : R = COC_6H_5

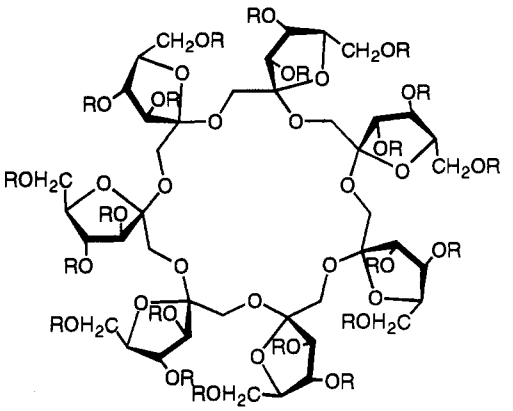

2

a : R = H
b : R = CH_3

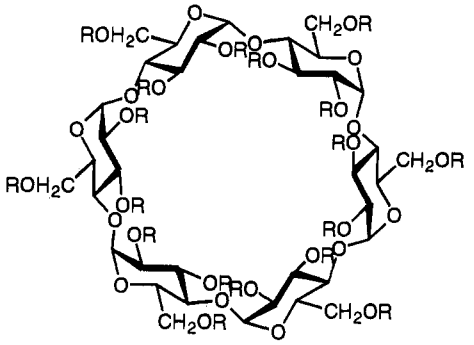

3

a : R = H
b : R = CH_3

standard host (H_{st}) which is usually added to an equimolar amount of the target host (H). Here, G^+ is a cationic guest,

$$H + (H_{st} + G)^+ \rightleftarrows (H + G)^+ + H_{st} \quad (1)$$

$$RPI = I[(H + G)^+]/I[(H_{st} + G)^+]$$

and $(H + G)^+$ and $(H_{st} + G)^+$ are the corresponding host–guest complex ions. $I[(H + G)^+]$ shows the peak intensity of the $(H + G)^+$ ion. Because permethylation enhances the sensitivity[15] and selectivity[13,14] of carbohydrates, such hosts have usually been utilized in FABMS.

Qualitative binding/interactions of the two isomeric hosts, permethylated cycloinulohexaose **1b** and permethylated α-cyclodextrin **3b**,[16] were compared using this RPI method. Their FAB mass spectral results are shown in Figure 1. *m*-Nitrobenzyl alcohol (NBA) was chosen as the matrix (mainly due to solubility problems), dibenzo-30-crown-10 as the internal standard host, and *n*-octylammonium ion as the cationic guest. Host **1b** exhibited

(12) (a) Fujii, I.; Isobe, R.; Kanematsu, K. *J. Chem. Soc., Chem. Commun.* **1985**, 405. (b) Beer, P. D. *J. Chem. Soc., Chem. Commun.* **1985**, 1115. (c) Miller, J. M.; Brown, S. J.; Theberge, R.; Clark, J. H. *J. Chem. Soc., Dalton Trans.* **1986**, 2525. (d) Bonas, G.; Bosso, C.; Vignon, M. R. *Rapid Commun. Mass Spectrom.* **1988**, *2*, 88. (e) Laali, K.; Lattimer, R. P. *J. Org. Chem.* **1989**, *54*, 496. (f) Miller, J. M.; Balasanmugam, K.; Fulcher, A. *Org. Mass Spectrom.* **1989**, *24*, 497. (g) Michaud, D. P.; Kyranos, J. N.; Brennan, T. F.; Vouros, P. *Anal. Chem.* **1990**, *62*, 1069. (h) Takayama, M.; Fukai, T.; Nomura, T.; Yamauchi, T. *Org. Mass Spectrom.* **1991**, *26*, 655. (i) Takahashi, T.; Uchiyama, A.; Yamada, K.; Lynn, B. C.; Gokel, G. W. *Tetrahedron Lett.* **1992**, 3825.

(13) (a) Sawada, M.; Ouyang, L.; Takai, Y.; Yamada, H.; Shizuma, M.; Kinoshita, T.; Mochizuki, T.; Hanafusa, T. *Bull. Chem. Soc. Jpn.* **1991**, *64*, 1243. (b) Sawada, M.; Shizuma, M.; Takai, Y.; Yamada, H.; Tanaka, T.; Okumura, Y.; Hidaka, Y.; Hanafusa, T.; Takahasi, S. *Bull. Chem. Soc. Jpn.* **1992**, *65*, 1275.

(14) (a) Sawada, M.; Shizuma, M.; Takai, Y.; Yamada, H.; Kaneda, T.; Hanafusa, T. *J. Am. Chem. Soc.* **1992**, *114*, 4405. (b) Sawada, M.; Okumura, Y.; Shizuma, M.; Takai, Y.; Hidaka, Y.; Yamada, H.; Tanaka, T.; Kaneda, T.; Hirose, K.; Misumi, S.; Takahashi, S. *J. Am. Chem. Soc.* **1993**, *115*, 7381. (c) Sawada, M. In *Biomedical Mass Spectrometry*; Matsuo, T., Seyama, Y., Caprioli, R., Gross, M., Eds.; John Wiley: New York, 1994; Chapter 3.19, p 639. (d) Sawada, M.; Okumura, Y.; Yamada, H.; Takai, Y.; Takahashi, S.; Kaneda, T.; Hirose, K.; Misumi, S. *Org. Mass Spectrom.* **1993**, *28*, 1525.

(15) (a) Dell, A.; Oates, J. E.; Morris, H. R.; Egge, H. *Int. J. Mass Spectrom. Ion Phys.* **1983**, *46*, 415. (b) Naylor, S.; Findeis, A. F.; Gibson, B. W.; Williams, H. *J. Am. Chem. Soc.* **1986**, *108*, 6359. (c) Poulter, L.; Burlingame, A. L. *Methods in Enzymology*; McCloskey, J. A., Ed.; Academic Press: San Diego, 1990; Vol. 193, p 661.

(16) (a) Ashton, P. R.; Stoddart, J. F.; Zarzycki, R. *Tetrahedron Lett.* **1988**, *29*, 2103. (b) Kurono, S.; Hirano, T.; Tsujimoto, K.; Ohashi, M.; Yoneda, M.; Ohkawa, Y. *Org. Mass Spectrom.* **1992**, *27*, 1157.

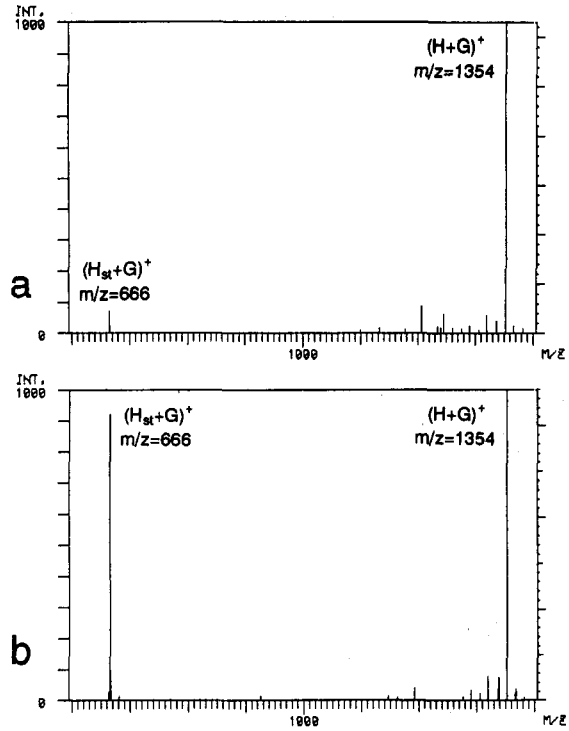

Figure 1. FAB mass spectra (NBA matrix). G^+ = *n*-octylammonium ion, H_{st} = DB-30-crown-10: (a) H = **1b** and (b) H = **3b**.

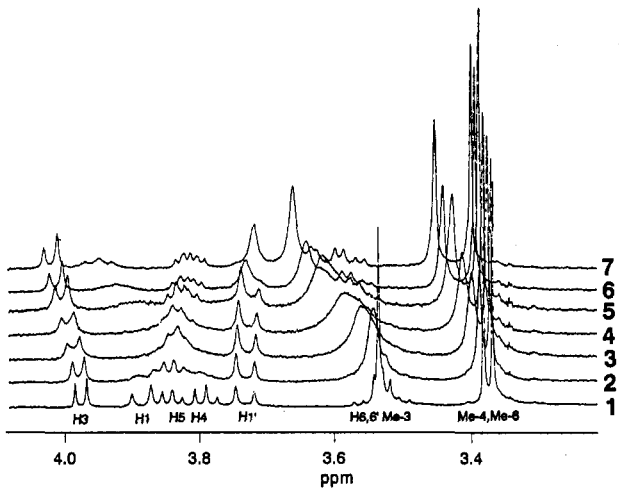

Figure 2. ^{1}H NMR spectral changes of **1b** with added KSCN in acetone-d_6 (298 K) ([**1b**]$_0$ = 5.71 × 10^{-4} M). Concentration of K^+: (1) 0, (2) 5.71 × 10^{-5}, (3) 1.71 × 10^{-4}, (4) 2.85 × 10^{-4}, (5) 4.54 × 10^{-4}, (6) 6.78 × 10^{-4}, (7) 1.01 × 10^{-3} M.

a much more intense peak of the 1:1 added ion [**1b**·$C_8H_{17}NH_3^+$] (RPI(**1b**) = 13.8) when compared with host **3b** (RPI(**3b**) = 1.1). Therefore, the high RPI ratio value (RPI(**1b**)/RPI(**3b**) = 12.5) observed suggests that **1b** binds the *n*-octylammonium ion more effectively than **3b**.[13,14]

NMR Spectral Analysis. Binding interactions of hosts **1b**, **2b**, and the related compounds with cations were mainly examined using ^{1}H NMR spectrometry.

^{1}H NMR spectral changes at 25 °C are shown in Figure 2, where a KSCN solution is successively added to a CD_3COCD_3 solution of **1b**. For assignment of the CH_3 protons in the spectra, the 2D NMR ($^3J_{CH}$, $^1J_{CH}$) technique was employed. On the other hand, alternative spectral changes are shown in Figure 3, where a $Ba(SCN)_2$ solution is added in a similar manner. Here, protons were assigned (as shown in Figure 3) using the saturation transfer technique or the 2D NOESY technique in a solution of **5** in Figure 3 (one

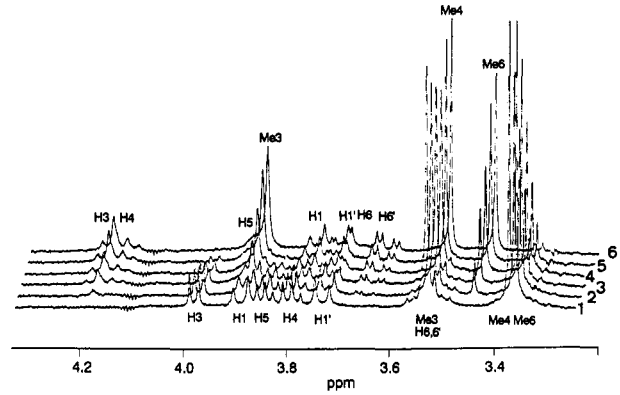

Figure 3. ^{1}H NMR spectral changes of **1b** with added $Ba(SCN)_2$ in acetone-d_6 (298 K) ([**1b**]$_0$ = 2.12 × 10^{-4} M). Concentration of Ba^{2+}: (1) 0, (2) 4.51 × 10^{-5}, (3) 1.12 × 10^{-4}, (4) 1.79 × 10^{-4}, (5) 2.68 × 10^{-4}, (6) 4.00 × 10^{-4} M.

of the exchange systems between **1b** and the corresponding barium complex [**1b**·Ba^{2+}]).

These two series of spectral changes are in contrast to each other. In the former case, resonance peaks shift gradually downfield or upfield as KSCN is added. This indicates that the exchange process between free host **1b** and its potassium complex [**1b**·K^+] is rapid when compared with the NMR time scale: time-averaged NMR shifts depending upon guest concentrations are observed.[17] On the other hand, in the latter case, original (free host, **1b**) peaks decrease and new resonance peaks (the corresponding complex, [**1b**·Ba^{2+}]) at higher or lower fields increase as $Ba(SCN)_2$ is added. This indicates that the corresponding exchange process is slow even at room temperature, compared with the NMR time scale, to give the distinct peaks of the barium complex ([**1b**·Ba^{2+}]).[17] Even in the K^+ ion complexation, such a slow exchange process can be successfully observed at much lower temperatures or in a $CDCl_3/CD_2Cl_2$ solvent (see following text). These results suggest that **1b** has an observable binding ability with K^+ or Ba^{2+} cation.

The other derivatives of **1a** such as the peracetylated derivative **1d** or the perbenzoylated **1e** resulted in practically no induced shift change by guest cation additions, even when an excess of KSCN or LiSCN solution was added. We assume that both hosts **1d** and **1e** have almost no binding activity with such cationic species probably due to severe steric hindrance for their complexations.

The permethylated cycloinuloheptaose **2b** provided observable induced shifts with K^+ ion additions, illustrating a sizable complexation ability.

Stoichiometry of the Complex and Association Constants. In the Ba^{2+} complexation system, concentrations of the complex [**1b**·Ba^{2+}] could be fortunately determined because the signals of the free host and its target complex were separately observed. Figure 4 shows a plot of the resulting [**1b**·Ba^{2+}] concentration versus the molar fraction of **1b** ($f_{(1b)}$),[18,19] where the conditions are kept constant at [**1b**] + [Ba^{2+}] = 3.8 × 10^{-3} M. The maximum concentration of the complex undoubtedly appears at $f_{(1b)}$ = 0.5. From this finding, the stoichiometry

(17) (a) Martin, M. L.; Martin, G. J.; Delpuech, J.-J. *Practical NMR Spectroscopy*; Heyden: London, 1980; Chapter 8. (b) Oki, M. *Application of Dynamic NMR Spectroscopy to Organic Chemistry*; VCH: Florida, 1985; Chapter 1.

(18) (a) Job, P. *Compt. Rend.* **1925**, *180*, 928. (b) Shibata, Y.; Inoue, B.; Nakatsuka, Y. *Nippon Kagaku Kaishi* **1921**, *42*, 983.

(19) Kikuchi, Y.; Kato, Y.; Tanaka, Y.; Toi, H.; Aoyama, Y. *J. Am. Chem. Soc.* **1991**, *113*, 1349.

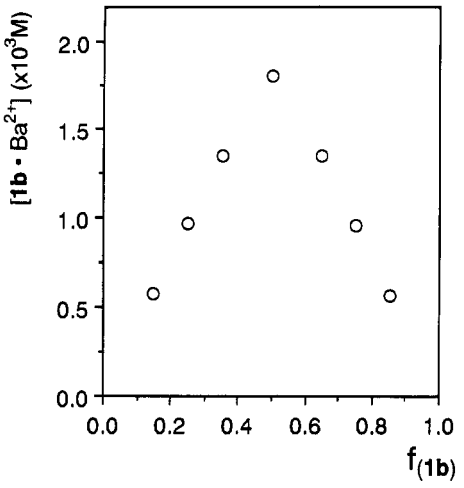

Figure 4. A Job plot of [1b·Ba^{2+}] vs mole fraction of **1b** ($f_{(1b)}$) in acetone-d_6 at 298 K ([**1b**] + [Ba^{2+}] = 3.84×10^{-3} M).

of the complexation between the host **1b** and the guest Ba^{2+} is confirmed as 1:1, at least in acetone solution.

The association constant (K_s) of **1b** with Ba^{2+} could be successfully determined by following the literature procedure[19] for these types of slow exchange systems. However, in the case of other rapid exchange systems, a ^1H NMR titration curve which is provided from a plot of induced shift versus concentration of guest added was analyzed by means of the so-called nonlinear curve fitting procedure.[14b,20,21] Here, the stoichiometry of all the complexations examined was assumed to be 1:1 for the calculations. The successfully calculated K_s values are summarized in Table 1. In most cases, spectra were followed until formation of the corresponding complex increased to approximately 50–70% complexation after successive guest additions. The downfield shifts of sharp signals assigned to methyl protons were mainly followed.

Inspection of Table 1 shows that K_s of **1b** with K^+ is 2 orders of magnitude smaller than that of 18-crown-6 with K^+ (for example, $K_s = 2.1 \times 10^4$ M^{-1} in 70% MeOH)[22] and K_s of **2b** with K^+ is still smaller than the former K_s by roughly 2 orders of magnitude.

Metallic Cation Selectivities. Figure 5 compares the dependencies of log K_s on metallic cation (radius) size for the three complexation systems of **1b** (in acetone), 18-crown-6 (in acetone),[23] and related calix[6]arene **4** (in acetonitrile).[24] The metallic cation selectivity of **1b** results in the order of $Li^+ < Na^+ < Cs^+ < K^+ < Ba^{2+}$ in acetone, and for the alkali metal ion series, the maximum occurs for K^+. This selectivity pattern is the same as that of the 18-crown-6[1] and is also in good accordance with that of **1a** reported using ligand-exchange thin-layer chromatography in aqueous solution.[5]

Compared with 18-crown-6, the characteristic features are simply noted as (i) smaller K_s for the Ba^{2+} complexation and (ii) larger K_s for the Li^+ one. As long as the comparison is limited to the mono cation series based on the similarities of the selectivity patterns, **1b** roughly lies between 18-crown-6 and calix[6]arene **4**, including the intermediately enhanced Li^+ behavior (Figure 5). These findings suggest that **1b** binds cations not in the central hole of the 18-crown-6 skeleton but nearly at the upper rim position. Judging from the crystal structure of **1a**,[4] the cation is possibly bound by three oxygens of the inner-type OMe group at the C-3 position of the fructofuranoses with a concurrent geometrical change in the 18-crown-6 skeleton: there are three alternative oxygens of the outer-type OMe-3 group which do not directly participate in the binding. The limiting induced shift values (simultaneously derived in the K_s determination process) support this view because the protons of Me-3 and Me-4 exhibit much larger complexation-induced downfield shifts.[25]

It is also noteworthy that the metallic cation selectivity of the larger 21-crown-7 macrocyclic host **2b** occurs in the order $K^+ < Cs^+$, showing a good agreement with that of **2a**.[5]

Rate Constant for Decomposition of the Potassium Complex [1b·K^+]. When a 0.6 equiv quantity of KSCN (1.15×10^{-3} M) was added to an acetonitrile solution of **1b** (1.96×10^{-3} M), all proton signals broadened (Figure 6b), showing the existence of a rather slow exchange process between **1b** and its potassium complex [1b·K^+] whose rate was close to the NMR time scale. When more KSCN (6 equiv; 1.24×10^{-2} M) was added, these peaks became sharp and shifted to a much greater extent (Figure 6c). This is due to the formation of the potassium complex. When the former solution (Figure 6b) was cooled to −40 °C, a significant spectral change was observed. Each methyl proton signal split into two singlets (Figure 6d), which corresponded to **1b** (○) and its potassium complex [1b·K^+] (△).

We noticed the broad Me-3 proton signal at 25 °C in Figure 6b (↓) and attempted to determine the rate constant (k_{-1}) for decomposition of the potassium complex [1b·K^+] using the exchange method (line-shape fitting method).[17] Under the conditions where the concentration ratio ([complex]/[free]) was 2/1 and the shift difference $\Delta\nu$ was 0.15 ppm, the k_{-1} was determined so as to reproduce the experimental half-width: because the Me-3 peak overlapped the H-6,6′ peaks, the k_{-1} was approximate. The decomposition rate constant (k_{-1}) of ca. 8×10^2 s^{-1} could be derived as a first-order approximation, and then k_1 was ca. 1×10^7 s^{-1} M^{-1} ($K_s = k_1/k_{-1} = 10^4$ M^{-1}).

Compared with the corresponding decomposition rate of 18-crown-6 ($k_{-1} = 49$ s^{-1} in MeOH)[26] or that of cryptand 222 ($K_{-1} = 1.8 \times 10^{-2}$ s^{-1} in MeOH),[27] that of **1b** ($k_{-1} = 8 \times 10^2$ s^{-1} in acetonitrile) seems to be relatively fast, suggesting that the potassium ion in the complex [1b·K^+] may not be bound more tightly than that in the other two complexes.

Charge-Induced Shifts. The complex ion structure was deduced by the method of induced-shift difference,[28] which uses a pair of $K^+(SCN^-)$ and Ba^{2+} (SCN^-_2) ions in acetone at 25 °C. Both cations have almost the same size

(20) (a) Diederich, F. *Angew. Chem., Int. Ed. Engl.* **1988**, *27*, 362. (b) Ferguson, S. B.; Diederich, F. *Angew. Chem., Int. Ed. Engl.* **1986**, *25*, 1127.

(21) (a) De Boer, J. A. A.; Reinhoudt, D. N.; Harkema, S.; Van Hummel, G. J.; De Jong, F. *J. Am. Chem. Soc.* **1982**, *104*, 4073. (b) Tsukube, H.; Sohmiya, H. *J. Org. Chem.* **1991**, *56*, 875.

(22) Izatt, R. M.; Terry, R. E.; Nelson, D. P.; Chan, Y.; Eatough, D. J.; Bradshaw, J. S.; Hansen, L. D.; Christensen, J. J. *J. Am. Chem. Soc.* **1976**, *98*, 7626.

(23) Boss, R. D.; Popov, A. I. *Inorg. Chem.* **1986**, *25*, 1747.

(24) Arnaud-Neu, F.; Collins, E. M.; Deasy, M.; Ferguson, G.; Harris, S. J.; Kaitner, B.; Lough, A. J.; McKervey, M. A.; Marques, E.; Rhul, B. L.; Schwing-Weill, M. J.; Seward, E. M. *J. Am. Chem. Soc.* **1989**, *111*, 8681.

(25) Ardini, A.; Pochini, A.; Reverberi, S.; Ungaro, R. *Tetrahedron* **1986**, *42*, 2089.

(26) Izatt, R. M.; Pawlak, K.; Bradshaw, J. S.; Bruening, R. L. *Chem. Rev.* **1991**, *91*, 1721.

(27) (a) Cox, B. G.; Garcia-Rosas, J.; Schneider, H. *J. Am. Chem. Soc.* **1981**, *103*, 1054. (b) Vögtle, F.; Weber, E. In *The Chemistry of Ethers, Crown Ethers, Hydroxyl Groups, and Their Sulphur Analogues*; Patai, S., Ed.; John Wiley: New York, 1980: Part 1, Chapter 2.

(28) Live, D.; Chan, S. I. *J. Am. Chem. Soc.* **1976**, *98*, 3769.

Table 1. Association Constants (M^{-1}) of 1b in Some Organic Solvents at 298 K[a]

host	guest A+	guest X-	solvent: acetone[b]	MeOH[c]	70% MeOH[d]	acetonitrile[e]
1b	Li^+	SCN^-	$(2.5 \pm 0.3) \times 10$ (6)			
1b	Na^+	SCN^-	$(1.5 \pm 0.3) \times 10^2$ (3)	$(2.6 \pm 0.2) \times 10$ (3)	0.6 ± 0.2 (2)	
1b	K^+	SCN^-	$(6.1 \pm 0.1) \times 10^3$ (2)		$(2.5 \pm 0.1) \times 10^2$ (2)	
1b	Cs^+	SCN^-	$(7.5 \pm 0.4) \times 10^2$ (4)	$(3.6 \pm 0.3) \times 10^3$ (3)		
1b	Ba^{2+}	SCN^-	1.9×10^4 (1)			
1b	NH_4^+	SCN^-	$(2.0 \pm 0.3) \times 10^2$ (5)		7.1 ± 0.3 (3)	
1b	$EtNH_3^+$	SCN^-	1.6 ± 0.2 (4)			$(1.9 \pm 0.6) \times 10$ (3)[f]
2b	K^+	SCN^-	$(2.9 \pm 0.8) \times 10$ (9)			
2b	Cs^+	SCN^-	$(7.1 \pm 1.1) \times 10$ (8)			

[a] Number of different protons followed by ^{1}H-NMR titration is in parentheses. [b] Acetone-d_6 (Wako 99.9%). [c] MeOH-d_4 (Aldrich 99.8% D). [d] MeOH-d_4/D_2O (v/v); D_2O (Wako >99.75%). [e] Acetonitrile-d_3 (Aldrich 99.5% D). [f] $EtNH_3PF_6$.

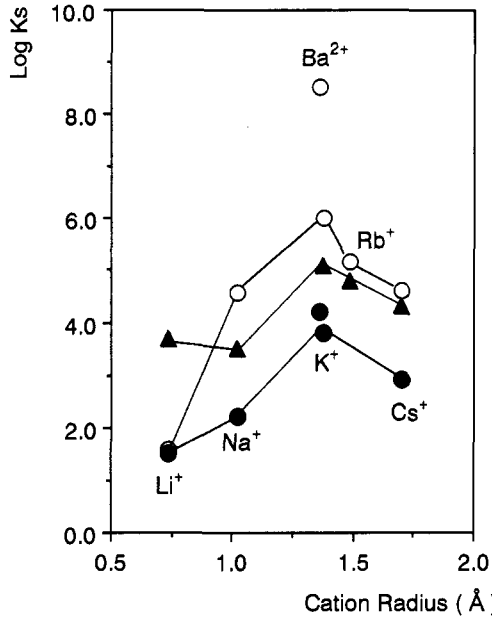

Figure 5. Log K_s vs cation radius plots for the complexations of **1b** (●), 18-crown-6 (○), and **4** (▲) with some metallic cations.

Chart 2

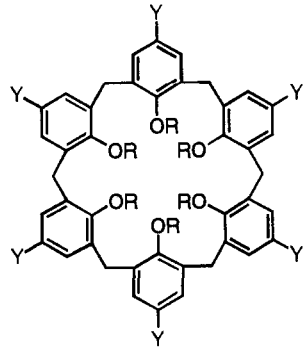

4

R = CH_2COOEt
Y = t-Bu

(r = 1.38 Å for K^+ and r = 1.36 Å for Ba^{2+}),[29] but different charge. Therefore, when the complexation geometry for the two complexes is assumed to be identical (see following text), the difference in the induced shifts [$\Delta\delta(Ba^{2+}) - \Delta\delta(K^+)$] will be able to cancel the contribution of the

(29) Lamb, J. D.; Izatt, R. M.; Swain, C. S.; Christensen, J. J. *J. Am. Chem. Soc.* **1980**, *102*, 475.

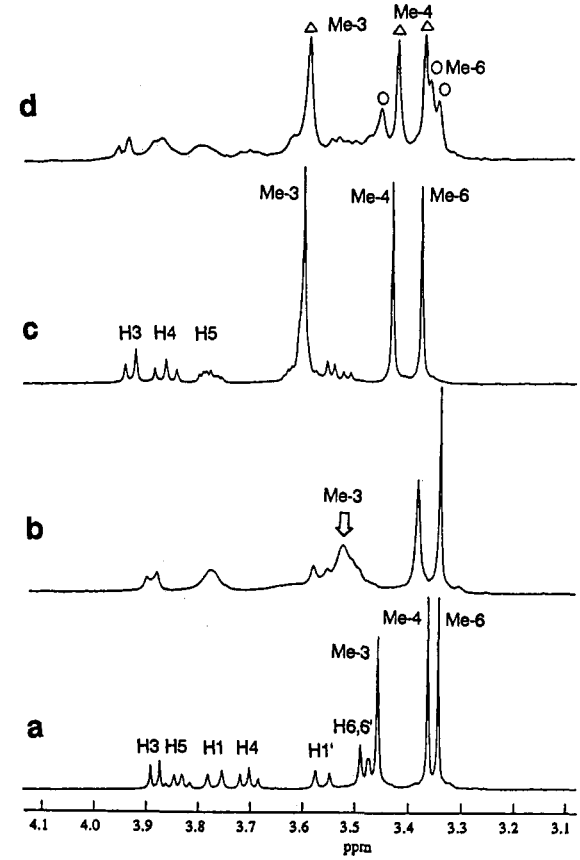

Figure 6. Temperature-dependent ^{1}H NMR spectra of **1b** with KSCN in acetonitrile-d_3: (a) [KSCN]/[**1b**] = 0 at 298 K, (b) [KSCN]/[1b] = 0.6 at 298 K, (c) [KSCN]/[**1b**] = 6.0 at 298 K, (d) [KSCN]/[**1b**] = 0.6 at 233 K.

complicated conformational (change) effect and hence evaluate that of the net charge-induced effect, which allows one to deduce the resulting complex ion structure. Table 2 shows the induced shift values by the K^+ or Ba^{2+} cation and the calculated charge-induced shift values.

It is interesting that the extent of the charge-induced shift of 0.19 ppm is the highest for the Me-3 proton. The methylene protons (H-1 and H-1′) of the central 18-crown-6 skeleton provide a much smaller value of 0.07 ppm as a simple average (0.14 and 0.0 ppm, respectively). On the other hand, the corresponding charge-induced shift of the same methylene proton for the 18-crown-6 itself provides 0.17 ppm. Accordingly, if K^+ was bound at the center of the 18-crown-6 skeleton of **1b** with a $g^+g^-g^+g^-g^+g^-$ conformation of the $-OCH_2CO-$ unit (D_{3d} symmetry),[30a] the charge-induced shift value would become much larger than 0.07 ppm. If a $g^+tg^+tg^+t$ conformation (C_3 symmetry) like the crystal structure of **1a**[4] was retained in the complex in solution, K^+ would not occupy such a central position

Table 2. Induced Shifts (ppm) of 1b by K^+ and Ba^{2+} and Charge Induced Shifts (ppm) in Acetone-d_6 at 298 K

host		induced shift (Δδ)		charge induced shift[a]
		K^+	Ba^{2+}	
1b	CH_2 H-1	−0.23	−0.09	0.14 } 0.07
	CH_2 H-1′	−0.01	−0.01	0.00 }
	H-3	0.05	0.21	0.16
	H-4	0.20	0.36	0.16
	H-5			ca. 0.09
	H-6, 6′			ca. 0.06
	Me-3	0.16	0.35	0.19
	Me-4	0.10	0.16	0.06
	Me-6	0.05	0.09	0.04
18-crown-6	CH_2	0.07	0.24	0.17

[a] Charge-induced shift is calculated by the difference of the two induced shift values [Δδ(Ba^{2+}) − Δδ(K^+)].

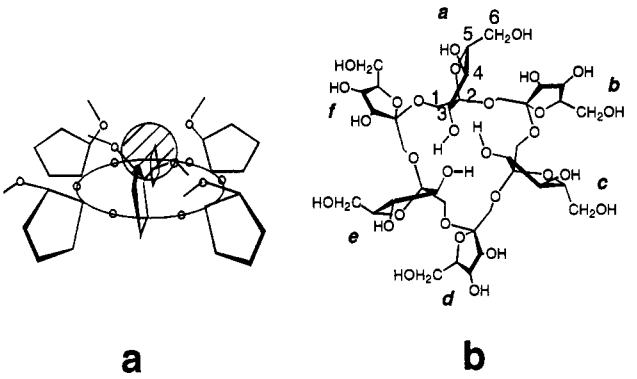

Figure 7. (a) An image drawing for an estimated structure of the complex between **1b** and a metallic cation. (b) An outlined crystal structure of **1a**.

on complexation because the methylene C–H bonds block the 18-crown-6 hole.[4] Therefore, we assume that **1b** binds the K^+ cation outside the 18-crown-6 hole, roughly using three oxygens of the inner type OMe-3 group (the upper rim of the molecule),[24,31] like the schematic image drawing in Figure 7a.

Temperature Dependencies of ^1H NMR and ^{13}C NMR Spectra. Temperature-dependent ^1H NMR spectra for a $CDCl_3/CD_2Cl_2$ (5/1) solution of **1b** and KSCN ([**1b**·K^+]/[**1b**] = 2/1) are shown in Figure 8. At −80 °C (193 K), three peaks of the complex [**1b**·K^+] (not of the free host **1b** at this temperature) clearly split into two peaks. The coalescence temperatures (T_c) correspond to ca. 200–220 K. These spectral changes suggest that the exchange rate between the two sites is relatively slow at such a lower temperature, and hence, the Me-3, Me-4, and Me-6 protons of the complex (○) are divided into two peaks in which one results from the inner-side occupied furanoses (for example, the *a*-, *c*-, *e*-furanoses in Figure 7b) and the other from the outer-side occupied ones (for example, the *b*-, *d*-, *f*-furanoses in Figure 7b in the crystal structure of **1a**).[4] Therefore, a possible complex structure in solution at lower temperature may be expected to have a structure with C_3 symmetry.

Figure 9 shows the temperature-dependent ^1H NMR spectral changes in a $CDCl_3/CD_2Cl_2$ (5/1) solution of the 100% barium complex [**1b**·Ba^{2+}] which is ensured by the addition of a sufficiently excess amount of $Ba(SCN)_2$.

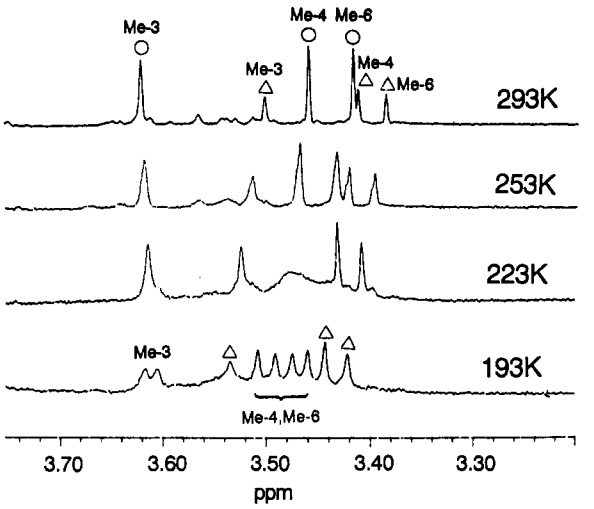

Figure 8. Temperature-dependent ^1H NMR spectra of **1b** with KSCN in $CDCl_3/CD_2Cl_2$ = 5/1 ([complex (○)]/[free(△)] = 2/1).

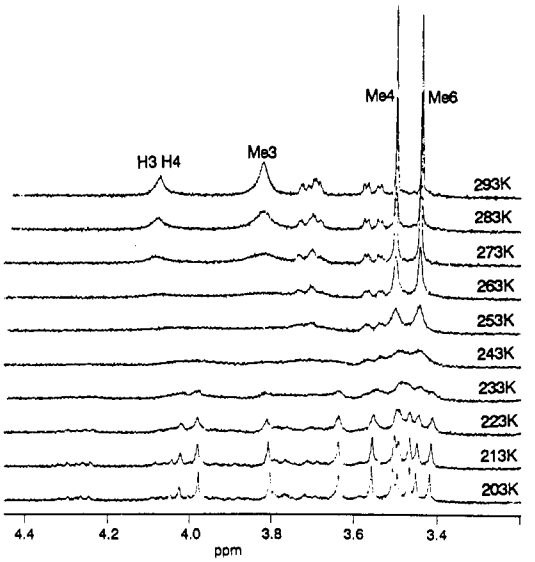

Figure 9. Temperature-dependent ^1H NMR spectra of **1b** with $Ba(SCN)_2$ in $CDCl_3/CD_2Cl_2$ (5/1).

Characteristically, all the methyl peaks split into three peaks (not into two) at −70 °C (203 K); the coalescence temperatures are ca. 230–260 K. Further, ^{13}C NMR spectra in an acetone solution of such a 100% barium complex showed similar changes (Figure 10). This NMR behavior is consistent with a structure showing C_2 symmetry. Such differences in symmetry of the complex structures (found by K^+ and Ba^{2+}) are not surprising because of the conformational flexibility of the target host **1b**. They are generally observed, and one of the typical examples is the crystal structures of 18-crown-6 with Na^+ (C_1 symmetry) and K^+ (D_{3d} symmetry),[30a,32,33] etc.[34]

Crystal Structure of the Complex [1b·Ba^{2+}]. As of now, no crystal structure has been available for a metal ion complex with **1b**: one crystal structure for **1a** is known.[4] From the interconnectivity with NMR spectrometric data in the solution-state complex,[1,6] the question arises of whether the metal cation is nestled or actually encapsu-

(30) (a) Seiler, P.; Dobler, M.; Dunitz, J. D. *Acta Crystallogr.* **1974**, *B30*, 2744. (b) We could not assign the atom (S or N in a counteranion). We tentatively use S in the present computation as the nearest atom in the counteranion (Figure 11).

(31) Shinkai, S.; Araki, K.; Kubota, M.; Arimura, T.; Matsuda, T. *J. Org. Chem.* **1991**, *56*, 295.

(32) Dunits, J. D.; Dobler, M.; Seiler, P.; Phizackerley, R. P. *Acta. Crystallogr.* **1974**, *B30*, 2733.

(33) Wipff, G.; Weiner, P.; Kollman, P. *J. Am. Chem. Soc.* **1982**, *104*, 3249.

(34) (a) Uiterwijk, J. W. H. M.; Harkema, S.; Feil, D. *J. Chem. Soc., Perkin Trans. 2* **1987**, 721. (b) Billeter, M.; Howard, A. E.; Kuntz, I. D.; Kollman, P. A. *J. Am. Chem. Soc.* **1988**, *110*, 8385.

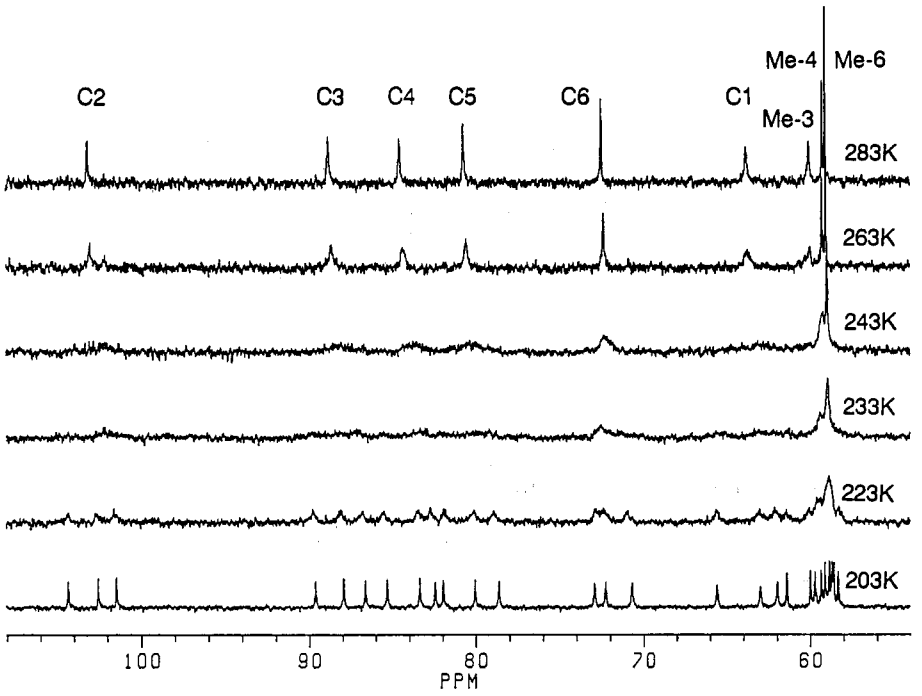

Figure 10. Temperature-dependent ^{13}C NMR spectra of **1b** with $Ba(SCN)_2$ in acetone-d_6.

Chart 3

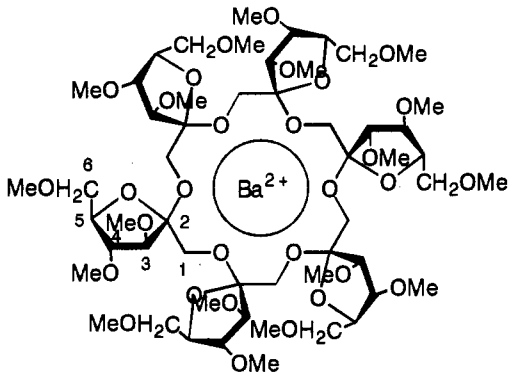

lated in the solid-state complex[35] in this macrocyclic 18-crown-6 derivative **1b** (Chart 3). The free host **1a** can be regarded as a kind of carbon-pivot lariat ether[36] because six furanose rings are intramolecularly involved in a spiro fashion in the macrocyclic crown ring.

The stereo drawings of the complex structure of **1b** with $Ba^{2+}(SCN)_2$ are shown in Figure 11 (non-H atoms only). A crystallographic 2-fold axis passes through the center of the molecule. The crystalline complex molecule demonstrates the following remarkable structural features.

(1) The Ba^{2+} cation is located at the nearest position to two OMe-3 oxygen atoms (Ba^{2+}···O; 2.86 Å) and is not nestled in the corresponding 18-crown-6 hole like the 18-crown-6 complexation with K^+ (D_{3d} symmetry, K^+···O; 2.81 Å average).[30a] This indicates unequivocal evidence for the OMe-3 oxygen participation in this binding architecture. Interestingly, the Ba^{2+} cation resides out of the 18-crown-6 plane; it is displaced to the opposite side to the 18-crown-6 oxygens from the O···O internuclear diagonal line.

In order to simply observe the arrangement of oxygen atoms around Ba^{2+}, a partial stereo drawing of the 18-crown-6 moiety as well as the four side-arm OMe-3 oxygens in the corresponding furanose rings is presented in Figure 12. The distances between Ba^{2+} and the 18-crown-6 oxygens are 2.94, 2.94, and 3.13 Å, providing an average value of 3.00 Å. As a coordination pattern around the Ba^{2+}, six oxygens in the crown ether moiety occupy a half-sphere, and four oxygens in the OMe-3 group (Ba^{2+}···O; 2.86 and 3.20 Å) (and probably one heteroatom in the SCN anion; 3.47 Å)[30b] occupy another half-sphere. As a consequence, the Ba^{2+} cation is displaced within a pocket formed by at least 10 oxygen atoms. The effective ionic radius has been reported as 1.52–1.57 Å for Ba^{2+} with 10–11 coordination numbers[35d] and the Ba^{2+}···O distance reported as 2.80–2.85 Å in the [Ba^{2+}·benzo-18-crown-6] complex.[9] The characteristic picture where oxygen atoms in the side arms are mainly used to bind a cation and then the cation does not occupy a center position in a macrocyclic ring is reminiscent of the complex structure of *N,N'*-bis(2-hydroxyethyl)diaza-18-crown-6 with Na^+,[35] etc.[37]

(2) The OMe-3 group in the furanose ring is classified into three types. They are (i) inner-near (Ba^{2+}···O; 2.86 Å), (ii) inner-moderate (Ba^{2+}···O; 3.20 Å), and (iii) outer (Ba^{2+}···O; 5.18 Å). The two oxygen atoms in the outer type cannot contribute to cation binding.

The C_2 symmetry in the solution complex [**1b**·Ba^{2+}] deduced from low-temperature NMR data completely agrees with that obtained in the crystalline complex. That is, the OMe-3 group of the complex is displaced non-equivalently at three different positions at low temperature and, as a consequence, is allowed to split into three peaks in both the ^1H and ^{13}C NMR spectra (Figures 9 and 10). The situation is the same for the other OMe groups and

(35) (a) Fronczek, F. R.; Gatto, V. J.; Schultz, R. A.; Jungk, S. J.; Colucci, W. J.; Gandour, R. D.; Gokel, G. W. *J. Am. Chem. Soc.* **1983**, *105*, 6717. (b) Gandour, R. D.; Fronczek, F. R.; Gatto, V. J.; Minganti, C.; Schultz, R. A.; White, B. D.; Arnold, K. A.; Mazzocchi, D.; Miller, S. R.; Gokel, G. W. *J. Am. Chem. Soc.* **1986**, *108*, 4078. (c) Fronczek, F. R.; Gandour, R. D. In *Cation Binding by Macrocycles: Complexation of Cationic Species by Crown Ethers*; Inoue, Y., Gokel, G. W., Eds.; Marcel Dekker: New York, 1990; Chapter 7, p 311. (d) Shannon, R. D. *Acta Crystallogr.* **1976**, *A32*, 751.

(36) Gokel, G. W. *Chem. Soc. Rev.* **1992**, 39.

(37) (a) Dang, L. X.; Kollman, P. A. *J. Am. Chem. Soc.* **1990**, *112*, 5716. (b) Doxsee, K. H.; Wierman, H. R.; Weakley, J. R. *J. Am. Chem. Soc.* **1992**, *114*, 5165.

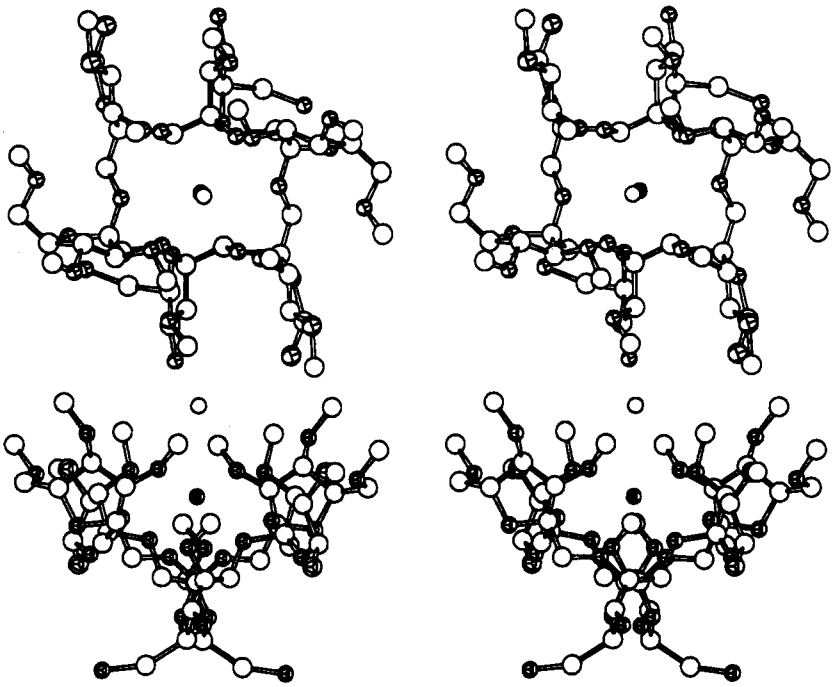

Figure 11. Stereodrawings of the crystalline complex [**1b**·Ba^{2+}][30b] (non-H atoms only): (top) a top view, (bottom) a side view. A barium cation is indicated as a black ball and oxygens as ellipses (the coordination is excluded for simplicity).

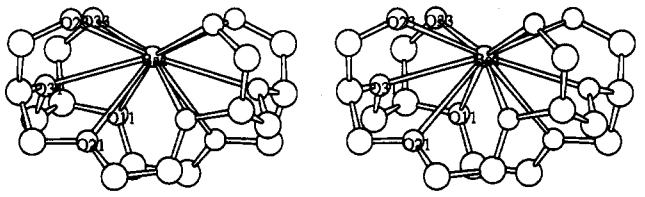

Figure 12. Partial stereodrawing of the crystalline complex [**1b**·Ba^{2+}]. The coordination of the Ba^{2+} ion is indicated: oxygens of the 18-crown-6 moiety and oxygens of OMe-3 in the furanose moiety: (Ba^{2+}···O_{11}) 2.94, (Ba^{2+}···O_{21}) 3.13, (Ba^{2+}···O_{31}) 2.94, (Ba^{2+}···O_{23}) 2.86, and (Ba^{2+}···O_{33}) 3.20 Å.

the interconnecting 18-crown-6 skeleton. Averaging phenomena at room temperature suggest up-and-down movements of each furanose ring and concurrent dynamic conformational changes in the backbone crown ether geometries.

As previously mentioned, the solution complex [**1b**·K^+] was deduced to have C_3 symmetry. Therefore, a change in the binding cation from K^+ to Ba^{2+} results in a change in the complex symmetry from C_3 to C_2. We assume that this symmetry change can be rationalized in terms of stronger electrostatic forces operating with Ba^{2+} than K^+. Such a different symmetry indicates a breakdown of the assumption mentioned before for the identical geometry of these two complexes. However, an important contribution of OMe-3 participations deduced from the induced shift method agrees with that for the solid-state structure of [**1b**·Ba^{2+}]. Therefore, this finding suggests the possibilities that different conformational contributions to the induced shifts are roughly cancelled in the methylene protons of the 18-crown-6 moieties and the corresponding OMe-3 participations are also important for the complex structure of [**1b**·K^+]. We hope to explore the solid-state structure in the future study.

(3) The six oxygens in the 18-crown-6 moiety are arranged in a twisted-boat structure (Figure 12).[35,37b] The conformation of the crown moiety is mainly represented by the arrangement of the torsion angles: $g^+ = 0 \sim +120°$, $g^- = 0 \sim -120°$, and $t = \pm 120 \sim 180°$. The arrangement of the OCCO torsion angles is $g^+g^+g^+g^+g^+g^+$ in the present complex [**1b**·Ba^{2+}] (cf., $g^+g^-g^+g^-g^+g^-$ in the complex [18-crown-6)·K^+]).[30a,33,34] Furthermore, the arrangement of the full sequential torsion angle is $(g^+ttg^+g^+tg^+g^+t)_2$ in the present complex [**1b**·Ba^{2+}] (cf., $(g^+ttg^-tt)_3$ in the complex [18-crown-6·K^+]).[30a,33,34] Because the Ba^{2+} cation sits outside the crown hole, this type of C_2 conformation (not D_{3d}) becomes favored for the crown ether geometry.

In conclusion, the new family of permethylated cycloinulohexaose **1b** can bind a barium cation within a pocket generated mainly by four OMe-3 oxygens in a total of six furanose rings and by the neighboring oxygens of the 18-crown-6 backbone with C_2 symmetry at least in the crystalline state and in the solution state at low temperature. The reduced cation binding abilities of this new class of carbohydrate host molecules **1b** and **2b** in the solution state at room temperature, compared with 18-crown-6, are reasonably concluded to result from this kind of complexation structure formed through a kind of induced fit binding mechanism with limited flexibility.

Experimental Section

Materials. Permethylated cycloinulohexaose (**1b**) was prepared from cycloinulohexaose (**1a**) by following the Hakomori method.[38] To a slight excess of dimethylsulfinyl carbanion which had been prepared from DMSO and NaH was added a solution of **1a** (1.0 g) in DMSO under N_2 with stirring. After being stirred for 4 h, the solution was cooled below 10 °C with an ice bath, and methyl iodide (10 mL) was slowly added. The mixture was allowed to stand at room temperature, and the stirring was continued overnight. After extraction with $CHCl_3$, the organic layer was washed with aqueous $Na_2S_2O_3$ and H_2O, dried over anhydrous $MgSO_4$, and evaporated in vacuo to afford **1b** as a colorless powder. The product was purified by resolidification from CH_2Cl_2/hexane (600 mg, 50% yield): mp 117–118 °C; FABMS (NBA matrix) m/z 1247 ((M + Na)$^+$); m/z 1354 ((M +

(38) (a) Hakomori, S. *J. Biochem.* **1964**, 55, 205. (b) Conrad, H. E. In *Method in Carbohydrate Chemistry*; Whistler, R. L., Bemiller, S. N. Eds.; Academic Press: New York, 1972; Vol. 6; p 361. (c) Melton, L. D.; McNeil, M.; Darvill, A. G.; Albersheim, P.; Dell, A. *Carbohydr. Res.* **1986**, *146*, 279.

$C_8H_{17}NH_3)^+$); FTIR (Nujol) 1128, 1103, and 1057 (ether CO) cm^{-1}. Anal. Calcd for $C_{54}H_{96}O_{30}$: C, 52.93; H, 7.90. Found: C, 53.08; H, 7.91. The corresponding deuterated compound, **1b**-d_{54} (**1c**), was similarly prepared using CD_3I: mp 100–101 °C.

Peracetylated cycloinulohexaose (**1d**) and the perbenzoylated derivative (**1e**) were prepared by the standard methods.[39] For **1d**, colorless crystals were obtained: mp 83–84 °C (64% yield); FTIR (Nujol) 1753 (C=O), 1228, 1045 (CO) cm^{-1}. Anal. Calcd for $C_{72}H_{96}O_{48}$: C, 50.00; H, 5.59. Found: C, 49.72; H, 5.42. For **1e**, recrystallization from CH_2Cl_2/hexane gave pale yellow crystals (78% yield): mp 104–105 °C; FTIR (Nujol) 1724 (C=O), 1267, 1176, 1109, 1068, 1026 (CO) cm^{-1}. Anal. Calcd for $C_{162}H_{132}O_{48}$: C, 68.35; H, 4.67. Found: C, 68.33; H, 4.56.

Cycloinuloheptaose (**2a**) was prepared from the enzyme digest of inulin by the methods described previously.[3a] The target carbohydrate was isolated from the digest by repeated chromatography with a column of QAE-Toyopearl 550C (Tosoh Corp., SO_4^{2-} form)[3a] and an eluent of 70% EtOH: fractions containing the carbohydrate were combined and evaporated to a syrup. EtOH was added to the syrup obtained and evaporated again. A colorless amorphous powder of **2a** was obtained: mp 164–166 °C.

Permethylated cycloinuloheptaose (**2b**) was prepared from cycloinuloheptaose (**2a**), as described above:[38] syrup, 71% yield; FABMS (NBA matrix) m/z 1467 ($(M + K)^+$); m/z 1558 ($(M + C_8H_{17}NH_3)^+$). Anal. Calcd for $C_{63}H_{112}O_{35}$: C, 52.93; H, 7.90. Found: C, 53.03; H, 7.63. Permethylated α-cyclodextrin (**3b**) was synthesized as reported previously[40] and recrystallized from CH_2Cl_2/hexane: mp 211–212 °C.

General Procedures. ^1H NMR spectra (360 MHz) and ^{13}C NMR spectra (90 MHz) were taken with a Bruker AM360 spectrometer: TMS was used as the internal standard except for the D_2O solvent (TSP).

FAB mass spectra (positive mode) were obtained with a JEOL DX300 mass spectrometer using a JMA3100 or JMA-DA6000 data processing system. The FABMS/RPI method[13,14] was employed, as in the case of the monosaccharides described before, where dibenzo-30-crown-10 was chosen as an internal standard host and NBA as a matrix. The concentration conditions in Figure 1a are the following. A methanolic solution of **1b** (0.1 M, 5 μL), a $CHCl_3$ solution of DB-30-crown-10 (0.1 M, 5 μL), a methanolic solution of *n*-octylammonium chloride (0.4 M, 5 μL), and NBA (20 μL) were mixed. After the solution was mixed with a vibrator, a 1-μL aliquot was deposited on a FAB probe tip. The resulting concentration ratio of $[H]:[H_{st}]:[G^+]$ was 1:1:4 ($[H] = 1.43 \times 10^{-2}$ M). Argon bombardment, a 5.0-s scan rate, and a 7.0-s data acquisition time were employed. Ten successive spectra (scans 15–25) were accumulated.

FTIR spectra were recorded with an Analect RFX-65 spectrometer. Elemental analyses were performed using Perkin-Elmer 2400 or 240C at the Material Analysis Center, ISIR, Osaka University. Liquid silica gel column chromatography was carried out on a Yamazen LC apparatus with an RI detector under appropriate medium pressure.

Determination of Association Constants. Association constants (K_s) were determined using ^1H NMR titration procedures as reported before:[14b] a nonlinear method was employed for the cases of $K_s > 3$ M^{-1} and a linear method (Benesi–Hildebrand equation) for the cases of $K_s < 3$ M^{-1}. Commercial samples of acetone-d_6, acetonitrile-d_3, and methanol-d_4 were used as solvents without purification.

The K_s values in Table 2 are the simple averages obtained from more than two different target protons which were followed by seven different guest concentrations: for example, for $K^+(SCN^-)$ guest with **1b** in acetone, $K_s = 5.97 \times 10^3$ M^{-1} (by following Me-4), 6.24×10^3 M^{-1} (by Me-6), and an average $K_s = (6.1 \pm 0.1) \times 10^3$ M^{-1}: the remaining Me-3 and the ring protons were not used for K_s calculations because of the exchange-broadened peaks. The concentration of host **1b** is 5.7×10^{-4} M. An acetone solution of KSCN was added to the host solution (NMR tube) using a microsyringe, and seven different guest concentrations (0 to 1.01×10^{-3} M) were employed: volume corrections were done for the calculation of host and guest concentrations. The solutions in the NMR tube were allowed to stand for ca. 15 min to approach and maintain the probe temperature (298 K). At the highest guest concentration, the chemical shift differences were $\Delta\delta^{max}_{Me-4} = 26.69$ Hz and $\Delta\delta^{max}_{Me-6} = 12.05$ Hz in these cases. For the complexation of $Ba^{2+}(SCN^-)_2$ guest with **1b** in acetone, the concentrations of both **1b** and its complex [**1b**·Ba^{2+}] were directly determined by integration of the corresponding ^1H NMR spectral peaks.

The commercial sample of Ba^{2+} salt ($Ba(SCN)_2 \cdot 2H_2O$) was used after drying in vacuo (with P_2O_5) at a temperature slightly higher than 40 °C for ca. 10 h. The other commercial SCN salts were freeze-dried and used without any purification. *n*-Octylammonium chloride was prepared from the corresponding amine. Ethylammonium thiocyanate (mp 43–44 °C) was prepared from the corresponding ammonium chloride.[41]

Crystal Structure Determination of the Complex [1b·Ba^{2+}]. Colorless crystals for X-ray crystallography were obtained by slow evaporation from an aqueous solution of **1b** and an excess amount of $Ba(SCN)_2$: crystal size, $0.50 \times 0.36 \times 0.55$ mm. Integral intensities were collected using graphite-monochromatized Mo Kα radiation ($\lambda = 0.710\,69$ Å) and an 11-kW rotating anode generator by the ω scan technique up to $2\theta_{max} = 60°$ (Rigaku AFC5FOS system). Of the 4244 unique reflections obtained, 1890 reflections ($F > 1.5\sigma(F)$) were used for the structure determination. The crystal data are the following: chemical formula, $C_{56}H_{96}N_2O_{30}S_2Ba$; formula weight, 1542.8; crystal system, tetragonal; space group, $P4_32_12$; cell dimensions, $a = 14.820(2)$ Å, $c = 33.132(5)$ Å, $V = 7276(1)$ Å^3; z 4; D_c 1.41 g/cm^3; R 16.2%.[45]

The structure was solved by direct methods (SHELXS86,[42] DIRDIF92)[43] and refined by full-matrix least-squares with anisotropic thermal parameters. All calculations were performed on an IRIS workstation with the teXsan crystallographic software package.[44] The final R value of 0.162 was not particularly precise probably due to large thermal vibration. In the present crystal structure, the positions of three carbon atoms (peripheral OMe type) and SCN groups (weak interaction with Ba^{2+})[30b] could not be determined: the SCN anions are presumed to interact weakly with the cation[30a] because of the encapsulation of the barium cation. However, the ORTEP views obtained demonstrate sufficient precision for the present structural discussion of the complex [**1b**·Ba^{2+}], especially for the position of the barium cation.

Acknowledgment. We are very grateful to Dr. Naoshi Imaki (Mitsubishi Kasei Co.) for the kind gift of **1a** and **1b** at an early stage of our work and to Mr. Hitoshi Yamada (MAC, ISIR, Osaka University) and Mrs. Fusako Fukuda (MAC, ISIR, Osaka University) for mass spectrometric and elemental analyses, respectively.

(39) (a) Boger, J.; Corcoran, R. J.; Lehn, J. M. *Helv. Chim. Acta* **1978**, *61*, 2190. (b) *Shinjikkenkagaku Koza*; Maruzen: Tokyo, 1978; Vol. 14; Chapter 10, p 2428. (c) Rogers, J. S.; Gutsche, C. D. *J. Org. Chem.* **1992**, *57*, 3152.

(40) Casu, B.; Reggiani, M.; Gallo, G. G.; Vigevani, A. *Tetrahedron* **1968**, *24*, 803.

(41) Curtis, W. D.; Laidler, D. A.; Stoddart, J. F.; Jones, G. H. *J. Chem. Soc., Perkin Trans. 1* **1977**, 1756.

(42) SHELXS86: Sheldrick, G. M. In *Crystallographic Computing 3*; Sheldrick, G. M., Kruger, C., Goddard, R., Eds.; Oxford University Press: Oxford, 1985; p 175.

(43) DIRDIF92: Beurskens, P. T.; Admirael, G.; Beurskens, G.; Bosman, W. P.; Garcia-Granda, S.; Gould, R. O.; Smits, J. M. M.; Smykalla, C. *The DIRDIF program system, Technical report of the crystallography laboratory*; University of Nijmegen: The Netherlands, 1992.

(44) teXsan: Crystal structure analysis package, Molecular Structure Corp., 1985 and 1992.

(45) The author has deposited atomic coordinates for [**1b**·Ba^{2+}] with the Cambridge Crystallographic Data Centre. The coordinates can be obtained, on request, from the Director, Cambridge Crystallographic Data Centre, 12 Union Road, Cambridge, CB2 1EZ, UK.